The International Journal of Advanced Manufacturing Technology (2019) 100:167–177
https://doi.org/10.1007/s00170-018-2716-0

ORIGINAL ARTICLE

A helical interpolation precision truing and error compensation for arc-shaped diamond grinding wheel

Jiahao Zhu [1,2] · Peng Yao [1,2] · Wei Wang [3] · Chuanzhen Huang [1,2] · Hongtao Zhu [1,2] · Bin Zou [1,2] · Hanlian Liu [1,2]

Received: 14 June 2018 / Accepted: 17 September 2018 / Published online: 22 September 2018

Abstract
In the grinding of aspherical optical surface, an arc-shaped diamond grinding wheel is generally employed, whereas its profile errors greatly influence the form accuracy of ground workpiece. A high efficiency helical interpolation precision truing method for the arc-shaped diamond grinding wheel is proposed in this paper. Helical interpolation trajectory and decreasing interpolation radius with the wear of a rotary truing wheel ensure a constant contact length and a uniform wear of the diamond grinding wheel and truer. The mathematical models of tool setting errors and measurement error of truer diameter in the truing process were established firstly. The prediction models considering the wear of truer are coincided well with the truing experiment results. Based on the mathematical error models, an error compensation truing process was proposed. The profile accuracy of an arc-shaped diamond grinding wheel was improved to 5 μm (PV) effectively by the error compensation truing process. An ellipsoidal surface of a fused silica workpiece was ground by the well-trued diamond grinding wheel. A form error (in PV) below 4.5 μm was obtained after precision grinding.

Keywords Aspheric lens · Ultra-precision grinding · Arc-shaped diamond grinding wheel · Form truing · Helical interpolation · Error compensation

1 Introduction

From the lens of a surgical endoscope and the camera lens of a mobile phone with a diameter of a few millimeters to the mirror of a ground-based space telescope with a diameter of several meters, aspheric lenses and mirrors with high form accuracy and surface quality, which leading to correcting of aberration and improving the image quality with fewer elements, have been widely used in advanced optical systems [1, 2]. Hard brittle materials such as optical glass and fine ceramics are ideal materials for aspheric lenses and mirrors because of their high refractive index, high hardness, good chemical stability, and corrosion resistance. Ultra-precision grinding is an ideal process for precision machining of hard brittle materials, which can give consideration to both of efficiency and accuracy [3]. However, inevitable wear of a diamond grinding wheel seriously affects the grinding accuracy [4], so the envelope grinding became a popular method for aspheric surface generation. Grinding points on the diamond grinding wheel are constantly changed in envelope grinding, which can effectively reduce the wear of the diamond grinding wheel and improve the grinding accuracy [5, 6]. However, there are various errors in the process of envelope grinding including tool setting error, machine positioning error, dimensional error, and profile error of a grinding wheel [7–9]. These errors can be eliminated by introducing many error compensation cycles in the grinding process, but it is very time consuming and may cost several days for a large aperture mirror [10]. Profile error of a grinding wheel has the greatest influence on grinding accuracy, which will be directly duplicated to the aspheric surface [11–13]. It can be removed by high efficient precision truing of the grinding wheel, which will

✉ Peng Yao
yaopeng@sdu.edu.cn

✉ Wei Wang
wangwei88@upc.edu.cn

[1] Center for Advanced Jet Engineering Technologies (CaJET), School of Mechanical Engineering, Shandong University, Jinan 250061, Shandong, China

[2] Key Laboratory of High Efficiency and Clean Mechanical Manufacture, Ministry of Education, PR China, Jinan 250061, Shandong, China

[3] College of Mechanical and Electronic Engineering, China University of Petroleum (East China), Qingdao 266580, Shandong, China

decrease compensation grinding cycles and increase machining efficiency dramatically. Therefore, it is necessary to find an effective truing method with high precision for the arc-shaped diamond grinding wheel.

In recent years, many researches focused on the precision truing of the arc-shaped diamond grinding wheel. The cup wheel was employed for truing arc-shaped grinding wheel by generating method, but a series of complex equipment were essential to achieve high accuracy [14]. A form truing method applying mutual wear between the diamond grinding wheel and GC stone was proposed [15]. Any required radius of wheel arc profile and non-circular profile could be obtained by this truing method, and truing devices were uncomplicated. However, because of that, the GC stone in this method was stationary, truing efficiency was low, and wear of the GC stone was serious. Then, an improved truing method was proposed, in which a rotary GC truing wheel is employed instead of the stationary GC stone [16]. The diamond grinding wheel was trued by the circular interpolation movement between the diamond and truing wheel. This method had a better truing efficiency and accuracy. However, the feed of the diamond grinding wheel along the axis of the truing wheel was not continuous in this method, which would leave grooves on the surface of the truing wheel. Due to this feeding mode, the abrasion of GC truing wheel during the circular interpolation movement would reduce the truing accuracy. What is more, errors existed in the truing process still need to be studied.

A precision helical interpolation truing method for the arc-shaped diamond grinding wheel is presented in this paper. The relative movement path between diamond grinding wheel and truing wheel is a helical line which can be performed by 3-axis linkage NC interpolation motion. The diamond grinding wheel has a velocity component along the generatrix of the truing wheel, which will improve the truing efficiency. The effects of abrasion of the truing wheel during the circular interpolation movement on the truing accuracy can be avoided by this feeding mode, and the wear of the truing wheel is uniform. Tool setting errors and the measurement error of truing wheel radius are investigated firstly. Mathematical models are established to predict the profile error after truing by considering the wear of truer. The prediction models considering the wear of GC truing wheel are coincided well with the truing experiment results. What is more, an error compensation truing process is proposed. At last, an ellipsoidal surface of the fused silica was ground by the well-trued diamond grinding wheel.

2 Truing principle

The stationary stone truing method [15] and circular interpolation method [16] are shown in Fig. 1a, b, respectively. Grinding grooves exist on the surface of the truing wheel after truing by these two feeding methods. During the stationary stone truing method, the contact length between the grinding wheel and truer increases with feeding in the depth direction, which will cause increase of truing force and lead to degrade of profile accuracy of grinding wheel. In the circular interpolation truing, the contact length is constant, but the raster scan interval must be very small to keep a small contact length, which will lead to very low truing efficiency. Intermittent contact between grinding wheel and dressing wheel in these two methods will cause nonuniform wheel surface quality.

The helical interpolation truing method is shown in Fig. 2. In this truing process, the diamond grinding wheel is tangent to the truing wheel, and the diamond grinding wheel has a helical interpolation movement along the truing wheel surface. That means that the diamond grinding wheel has a circular interpolation movement in the y-z plane, and it has a continuous and reciprocating feeding motion along the x-axis synchronously. The movement path of the diamond grinding wheel is shown in Fig. 2. The grinding wheel and truer keep contact continuously and the contact length is constant, which will lead to uniform wheel surface quality and high wheel profile accuracy. The truing efficiency can be dramatically improved by increasing the feed rate.

These two wheels have different rotational speeds, and the profile of arc-shaped wheel will be achieved through the mutual wear between grinding wheel and truing wheel. In this paper, the process of a reciprocating helical interpolation movement of the diamond grinding wheel is defined as one truing cycle. After every truing cycle, the grinding wheel feeds a depth of a_p along the radius of the circular interpolation in the y-z plane. In each truing cycle, every point on the surface of the truing wheel takes part in the truing process, which thus avoids the effect of the truing wheel wear on the truing accuracy in this cycle. The constant contact length between the truer and grinding wheel arc keeps a constant truing force during the whole process which also benefits the improvement of truing accuracy.

The geometric relationship between the diamond grinding wheel and the truing wheel is shown in Fig. 3. The radius of the circular interpolation in the y-z plane, R, can be described as Eq. 1.

$$R = r + r_1 \tag{1}$$

where r is the expected radius of the wheel arc profile and r_1 is the initial radius of the truing wheel. The arc profile of grinding wheel with any required radius can be obtained by changing the radius of the circular interpolation. The truing wheel radius will be reduced a_p after each truing cycle. Thus, the radius of the circular interpolation after each truing cycle R' may be calculated as follows,

$$R^{'} = R - a_p \tag{2}$$

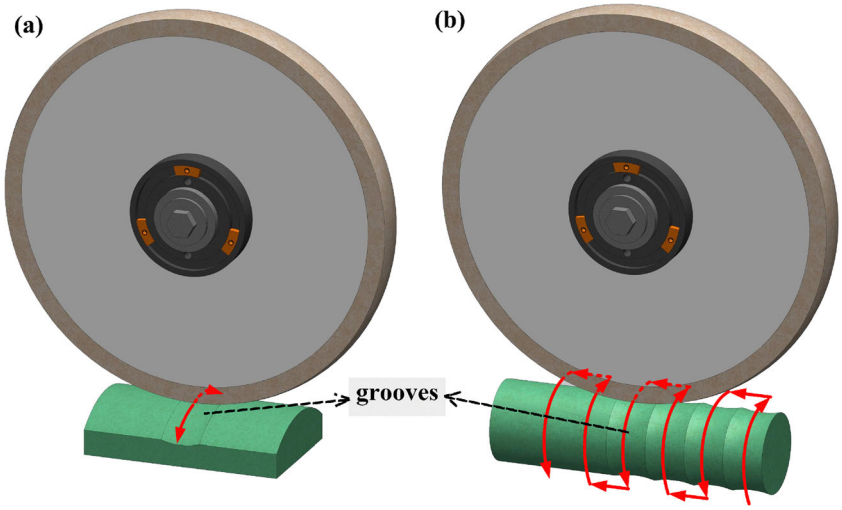

Fig. 1 Schematic of **a** stationary stone truing method and **b** circular interpolation truing method

where a_p is the grinding depth of the diamond grinding wheel. In the truing process, the two limiting positions of the contact between the diamond grinding wheel and the truing wheel are point a and point b. The distance between these two points, B_1, can be described as:

$$\frac{r}{B} = \frac{r_1}{B_1} \tag{3}$$

where B is the width of the diamond grinding wheel. According to the geometric model in Fig. 3, the influence of tool setting errors and measurement error of truer radius on the profile error of grinding wheel arc are analyzed in the part 4 of this paper.

3 Experimental

3.1 Design of experiments

The experimental process is shown in Fig. 4. Firstly, the effects of tool setting errors of z axis and y axis and the measurement error of truing wheel radius on truing accuracy were investigated, respectively. The mathematical models of these three errors existed in truing process that was established to predict the profile error after truing. Truing experiments were conducted, and appointed errors were artificially introduced in truing process. The experimental results were compared with the predicted results in order to verify the accuracy of the prediction models. Based on these mathematical models, an

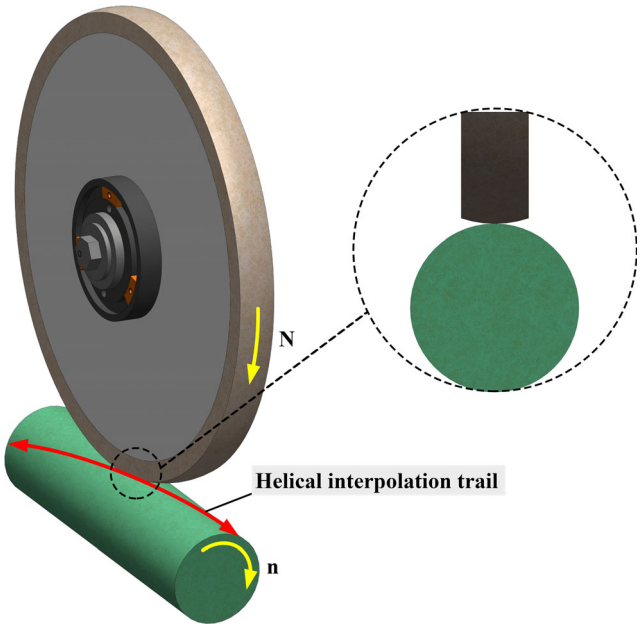

Fig. 2 Schematic of the helical interpolation precision truing method

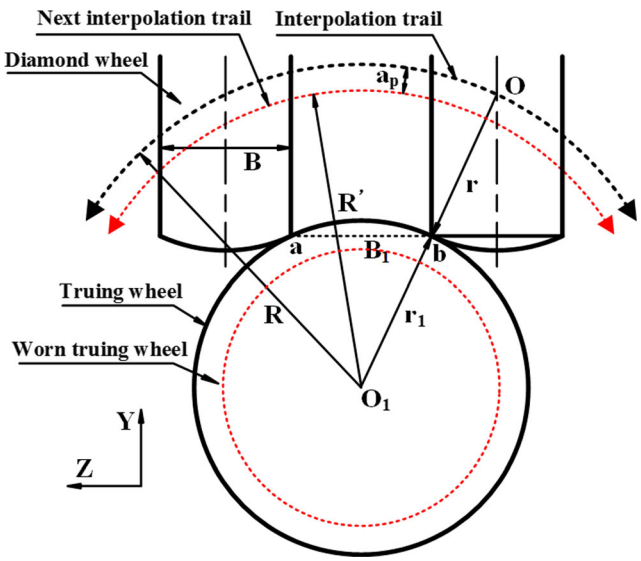

Fig. 3 Geometric relation between the diamond grinding wheel and the truing wheel

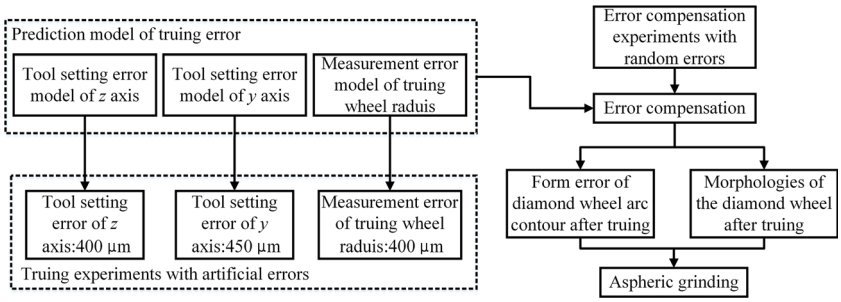

Fig. 4 Schematic of experimental process

error compensation method was proposed and error compensation truing experiments were conducted. In the error compensation experiments, the errors existed in truing process were random and not intervened artificially. The profile errors of the wheel arc profile and surface topographies of the diamond grinding wheel were measured after truing. At last, aspheric grinding experiments for the ellipsoidal surface of fused silica were performed utilizing the well-trued diamond grinding wheel.

3.2 Setup and parameters of experiments

The precision truing and aspherical grinding experiments were performed on a 3-axis CNC ultra-precision grinder NAS520-CNC, which is shown in Fig. 5, through 3-axis linkage NC interpolation motion. The wheel arc profile was measured by the Keyence LK-G10 laser displacement sensor while the grinding wheel was rotating, as shown in Fig. 6a. The envelope curve of measured profile was used to represent the profile of the diamond wheel in the grinding process. Surface morphologies of the diamond grinding wheel were measured by Keyence VK-X200, a confocal laser scanning microscope(CLSM), as shown in Fig. 6b. After truing, surface morphologies of the diamond grinding wheel were duplicated by the vinyl polysiloxane impression. Then, the impression was measured by the CLSM after duplication. Surface morphologies of the diamond grinding wheel could be obtained by reversing the height data.

The parameters of the diamond grinding wheel and truing wheel used in the truing experiments are shown in Table 1. 180# (average grain size of 90 μm) GC (green silicon carbide) truing wheel was chosen to be the truer for the 120# (average grain size of 125 μm) diamond grinding wheel, because the truing efficiency is the highest when the grain sizes of the diamond grinding wheel and GC truing wheel are similar, meanwhile smaller grains of the truing wheel will improve truing accuracy. The truing parameters are shown in Table 2.

An ellipsoidal surface of the fused silica was then ground by the well-trued 120# resinoid bond diamond grinding wheel through the error compensation truing process we proposed. The setup of grinding experiments is shown in Fig. 7. The fused silica workpiece used was ground by parallel grinding method. The detail information about grinding wheel, aspheric workpiece, grinding conditions, and parameters is shown in Table 3. The form error of the fused silica workpiece was measured by scanning along the Z axis direction on-machine with the laser displacement sensor before and after grinding.

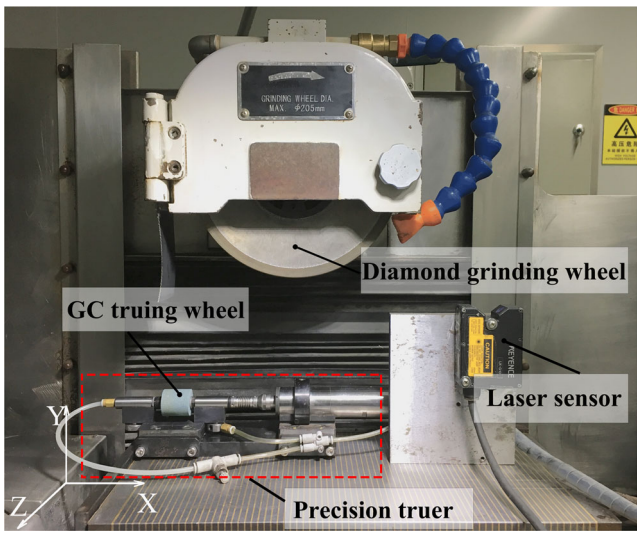

Fig. 5 Setup of truing experiments

4 Results and discussion

4.1 Analysis of errors in truing process

4.1.1 Analysis of the tool setting error of *z* axis

The relative position relationship between the grinding wheel and the truing wheel in z axis is established through conducting the lateral surface of grinding wheel to contact with the edge of the lateral surface in truing wheel. In the tool setting process of z axis, the possible error is that the diamond deviates from the ideal position along the positive or negative direction of z axis. If the diamond grinding wheel deviates to the negative direction of z axis and the value of deviation is Δz, the actual truing condition is shown in Fig. 8a. Due to the tool setting error of z axis, the material removal volume of the left

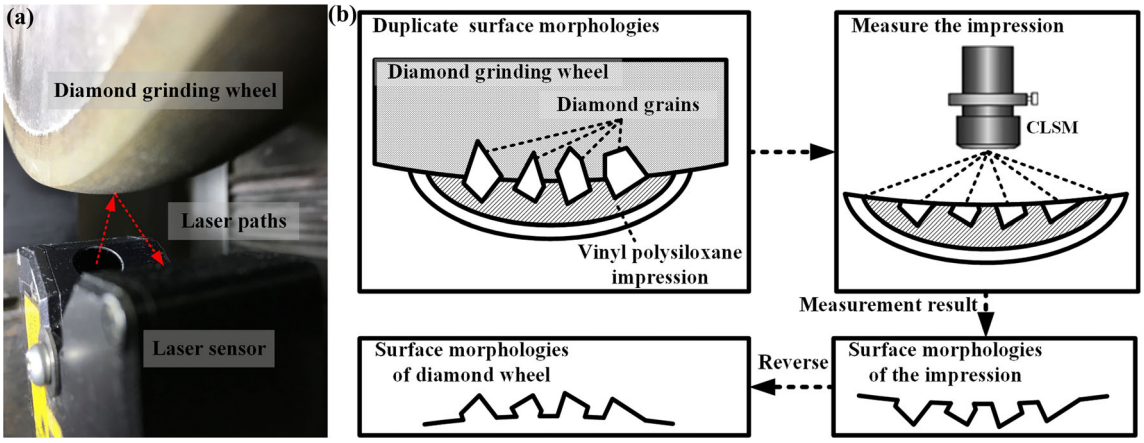

Fig. 6 Measurement of **a** profile of wheel arc, **b** surface morphologies of wheel surface

side of wheel arc profile is larger than the ideal value; meanwhile, the material removal volume of the right side is smaller. The corresponding central angle of these two parts is θ_1 and θ_2, which can be described as Eq. 4 and Eq. 5.

$$\theta_1 = \alpha_1 - \alpha_2 = sin^{-1}\frac{B/2}{r} - sin^{-1}\frac{\Delta z/2}{r_1} \tag{4}$$

$$\theta_2 = \alpha_1 + \alpha_2 = sin^{-1}\frac{B/2}{r} + sin^{-1}\frac{\Delta z/2}{r_1} \tag{5}$$

The normal deviation along the radius direction at point $P(x, y, z)$ which is on the actual diamond grinding wheel arc profile is defined as $e_z(P)$. Supposing that the truing wheel is not worn in the truing process, the law of deviation $e_z(P)$ varying with z coordinates can be described as Eq. 6.

$$e_z(P) = r_1 - \sqrt{r_1^2 + \Delta z^2 - 2\Delta z\left(\frac{r_1}{r}Z - \frac{B}{2}\right)} \tag{6}$$

For example, when the tool setting error of z axis was set to 400 μm, profile error after truing was compared with the predicted error without considering truer wear in Fig. 8b. The error prediction model expressed by Eq. 6 was established by supposing that only material on the diamond grinding wheel surface is removed, while the wear of the truing wheel was ignored. Actually, the truing wheel and diamond grinding wheel were worn at the same time. Hence, there was a disparity between the experimental and predicted result. According to the experimental results, an abrasion correction factor was introduced to the prediction model. Then, $e_z(P)$ can be described as follows after correction,

$$e_z(P) = t^* * \left(r_1 - \sqrt{r_1^2 + \Delta z^2 - 2\Delta z\left(\frac{r_1}{r}Z - \frac{B}{2}\right)}\right) \tag{7}$$

where t^* is the abrasion correction factor.

The abrasion correction factor t^* means the ratio of radial wear of the diamond wheel and truing wheel during the truing process. It is affected by many truing parameters, including the feeding rate, the rotation speed, and the grain sizes of the diamond wheel and truing wheel. Its value can be obtained by measuring the radii reduction of the diamond grinding wheel and the truing wheel after a truing process. According to the experimental results, the value of t^* is 0.22. As shown in Fig. 8b, the experimental results coincided well with the prediction model after correction. And average deviation between them was 1.926 μm, which may be caused by other unavoidable errors existed in truing process, e.g., the positioning error of machine tool. It can be seen that the shape of profile error curve is approximated to a straight line when the tool setting error of z axis exists. The material removal volume of the grinding wheel profile decreases linearly alone the z direction.

Table 1 Parameters of the diamond grinding wheel and truing wheel

	Parameters	
Diamond grinding wheel	Bond	Resin bond
	Grain size	125 μm
	Diameter	D = 205 mm
	Width	B = 12 mm
	Radius of wheel arc profile	r = 25 mm
GC truing wheel	Grain size	90 μm
	Length	L = 25 mm
	Radius	r_1=20 mm

Table 2 Truing parameters

Speed of the diamond grinding wheel (rpm)	Speed of the truing wheel (rpm)	Feed rate (mm/min)	Depth of cut (μm)
800	2000	240	2

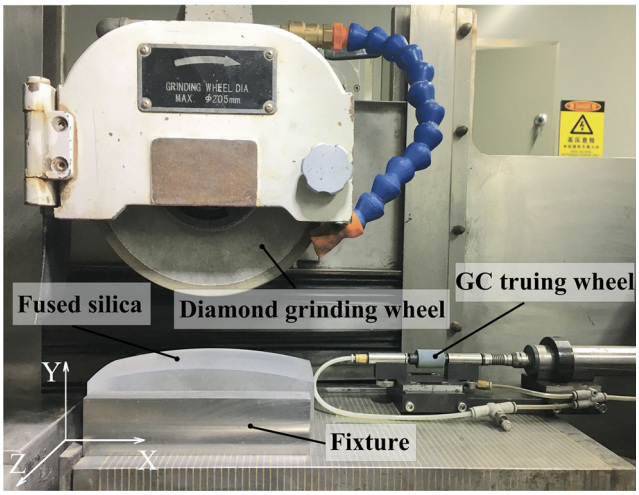

Fig. 7 Setup of grinding experiments

4.1.2 Analysis of the tool setting error of *y* axis

The relative position relationship between the grinding wheel and truing wheel in y axis is established through conducting the lowest point in the arc profile of the grinding wheel to contact with the highest generatrix in truing wheel. The possible error in the tool setting process of y axis is that the grinding wheel deviates from the ideal position along the negative direction of y axis. Figure 9a shows the actual truing condition. Due to the tool setting error of y axis, the material removal volume of wheel arc profile is larger than ideal value. And the material removal volume gradually decreases from the middle to the edge of wheel arc profile. The arc profile of the diamond grinding wheel will be symmetrically after truing. If the value of deviation is Δy, the law of deviation $e_y(P)$ varying with z coordinates can be described as Eq. 8.

$$e_y(P) = r_1 - \sqrt{r_1^2 + \Delta y^2 - 2\Delta y\sqrt{r_1^2 - \left(\frac{r_1}{r}Z - \frac{B}{2}\right)^2}} \tag{8}$$

Consider with the abrasion correction factor, the law of deviation $e_y(P)$ varying with z coordinates can be described as,

$$e_y(P) = t^* * \left(r_1 - \sqrt{r_1^2 + \Delta y^2 - 2\Delta y\sqrt{r_1^2 - \left(\frac{r_1}{r}Z - \frac{B}{2}\right)^2}} \right) \tag{9}$$

where t^* is 0.22.

When the y axis tool setting error was set to 450 μm, the experimental results and prediction model of profile error after truing are compared in Fig. 9b. The predicted error curve after correction by abrasion correction factor and the experimental curve were almost coincident, and average deviation between them is 1.043 μm. It can be found that the error curve is axisymmetric, and material removal volume of grinding wheel gradually decreases from the middle to the edge of wheel arc profile when tool setting error of y axis exists.

4.1.3 Measurement error of the truing wheel radius

Measured value of the truing wheel radius may be larger or smaller than the actual value. According to Eq. 1, if the measured truing wheel radius is r_1' which is smaller than the actual value, the radius of the circular interpolation R can be calculated as,

$$R = r + r_1' = r + r_1 - \Delta r \tag{10}$$

where Δr is the deviation between the measured truing wheel radius and the actual value. What is more, in the process of tool setting, appropriate deviation Δz and Δy will occur in the direction of z and y axis due to the measurement error of the truer radius.

$$\Delta z = \Delta r \tag{11}$$

$$\Delta y = \Delta r - r_1 + \sqrt{r_1^2 - \Delta r^2} \tag{12}$$

Table 3 Grinding conditions and parameters

Items		Parameters
Grinding wheel		120# resinoid diamond grinding wheel
Workpiece	Material	Fused silica
	Length	150 mm
	Width	70 mm
	Thickness	50 mm
Aspheric equation		$z = \frac{-r^2}{377.3 + \sqrt{377.3^2 - 0.2 \times r^2}}$
Grinding method		Parallel grinding, Axial-feed grinding
Depth of cut		5 μm, 1 μm
Speed of the diamond grinding wheel		1500 rpm
Feed speed		450 mm/min

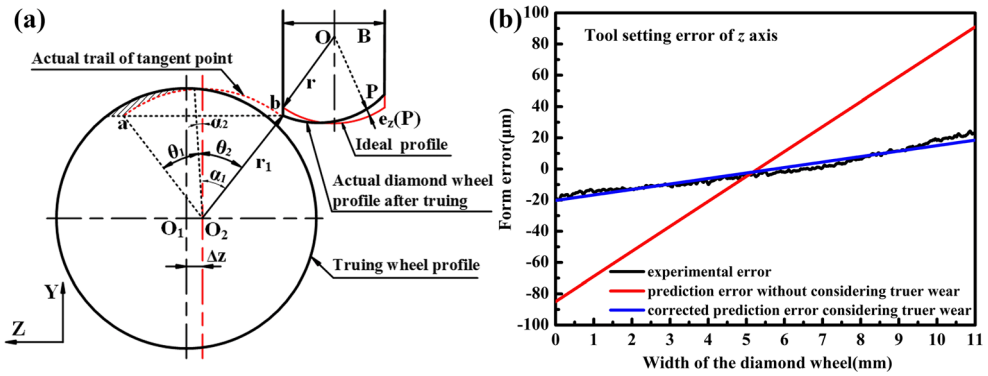

Fig. 8 **a** Schematic of the actual truing condition with tool setting error of z axis. **b** Comparison between prediction and experimental profile error curves

The actual truing condition is shown in Fig. 10a. Due to the measurement error, the material removal volume of the left side of wheel arc profile is smaller than ideal value; meanwhile, the material removal volume of the right side is larger. The corresponding central angle of these two parts are identical. If the value of the measurement error is Δr, the law of deviation $e_r(P)$ varying with z coordinates can be described as Eq. 13.

$$e_r(P) = r_1 - \sqrt{\left(\frac{r_1}{r}Z - \frac{B}{2} + \Delta r\right)^2 + \left[\sqrt{(r_1-\Delta r)^2 - \left(\frac{r_1}{r}Z - \frac{B}{2}\right)^2} + \Delta r - r_1 + \sqrt{r_1^2 - \Delta r^2}\right]^2} \tag{13}$$

Considering the abrasion correction factor, the law of deviation $e_r(P)$ can be described as,

$$e_r(P) = t^* * \left(r_1 - \sqrt{\left(\frac{r_1}{r}Z - \frac{B}{2} + \Delta r\right)^2 + \left[\sqrt{(r_1-\Delta r)^2 - \left(\frac{r_1}{r}Z - \frac{B}{2}\right)^2} + \Delta r - r_1 + \sqrt{r_1^2 - \Delta r^2}\right]^2}\right) \tag{14}$$

where t^* is 0.22.

As shown in Fig. 10b, when the measurement error of the truing wheel radius was 400 μm, profile error of the diamond grinding wheel arc profile after truing is compared with the predicted value. After correction of the predicted error curve, average deviation between these two curves was 2.706 μm. It can be seen that the slope of error curve is gradually increasing when measurement error of the truing wheel radius exists.

4.2 Error compensation

According to the above analysis, due to the tool setting errors and measurement error of the truing wheel's radius, it is hard to obtain a satisfactory form accuracy of wheel arc profile by a single truing process. The higher form accuracy can be obtained through error compensation truing processes.

Based on the error prediction models, an error compensation method was proposed, as shown in Fig. 11. The type of error that existed in truing process could be judged by the truing error curve. Then, the compensation value could be inversely calculated by the prediction models. According to the calculated compensation value, the relative zero point of coordinates or the interpolation radius in the CNC program will be adjusted.

There may be a variety of errors at the same time in actual truing process. To compensate the errors, they should be decoupled through error analysis. Wheel profile error curves

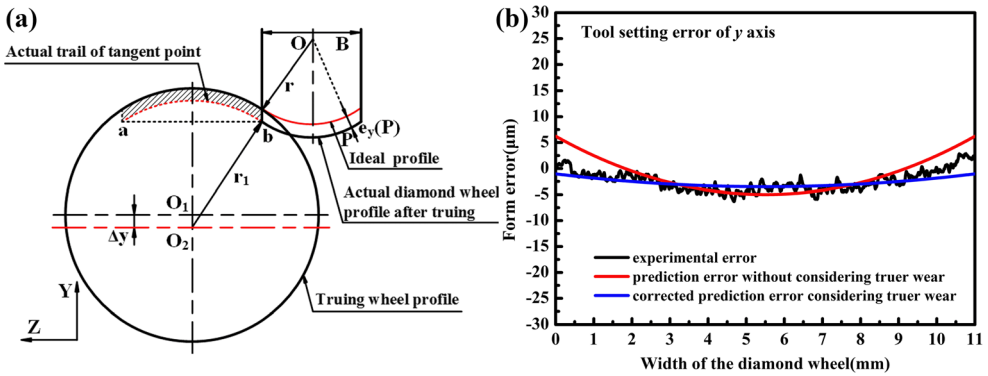

Fig. 9 **a** Schematic of the actual truing condition with tool setting error of y axis. **b** Comparison between prediction and experimental profile error curves

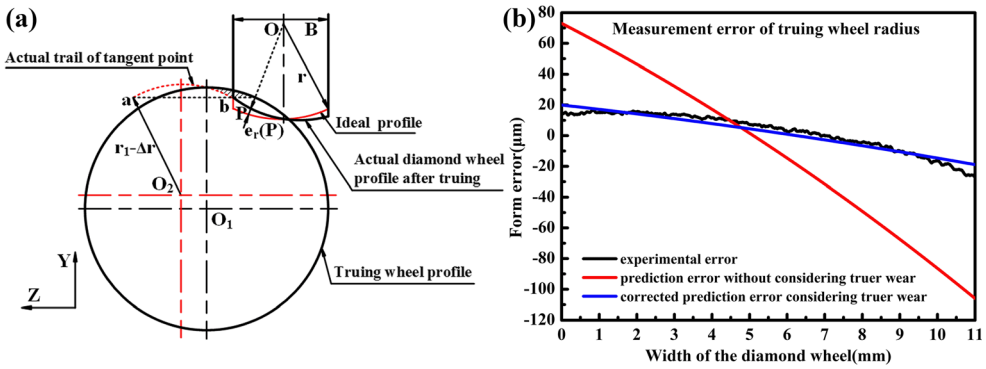

Fig. 10 **a** Schematic of the actual truing condition with measurement error. **b** Comparison between prediction and experimental profile error curves

of difference stage of the error compensation truing experiments are shown in Fig. 12. Figure 12a shows an error curve after the first truing cycle. This curve is approximatively sinusoidal curve with a slope, which is out of accord with the above three kinds of error curves. It can be considered that there were two or more composite truing errors exist in the truing process. In Fig. 12a, material removal volume in the middle area of wheel arc profile gradually increases linearly. According to the prediction model of tool setting error of z axis, it can be judged that the tool setting error of z axis may exist in the truing process. Therefore, least squares algorithm is used to fit the error curve according to Eq. 7. Meanwhile, the value of tool setting error of z axis existed in truing process was resolved, which is 127 μm. It means that this part of error can be removed by a compensation truing process after adjusting the z axis reference point by 127 μm along the negative direction. The predicted residual error curve after this compensation truing process is shown as the red curve in Fig. 12b. According to the error compensation scheme, the tool setting error of z axis was compensated in next truing cycle.

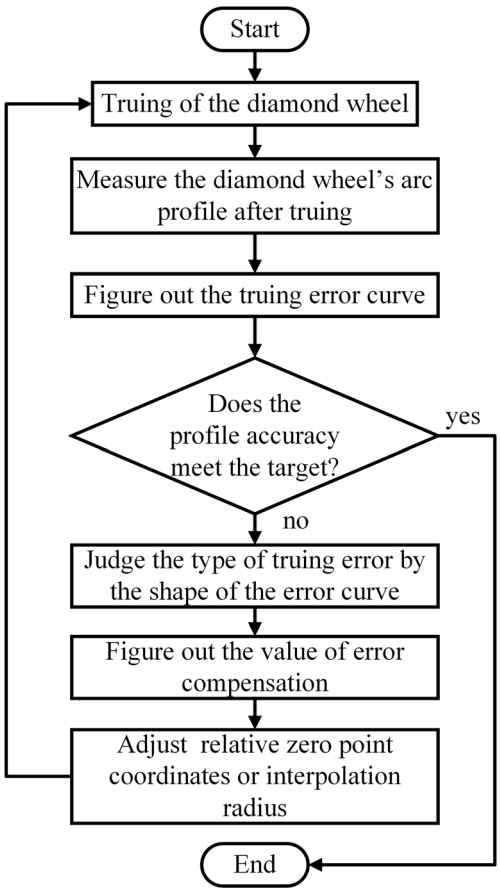

Fig. 11 Flow chart of error compensation scheme

The actual residual error curve after the second truing cycle is shown as the black curve in Fig. 12b. It can be seen that the red and the black error curves in Fig. 12b show same trends, and the profile accuracy of grinding wheel profile was improved, but further compensation should be conducted. The actual residual error curve shows that the material removal volume of the right side of wheel arc profile gradually decreases, and the slope of error curve is gradually increasing. This curve is similar with the prediction model of measurement error of truing wheel radius, so it can be partially removed by another compensation truing process after setting a smaller radius of wheel arc. Using the same fitting method mentioned in the compensation of z axis setting error, the value of the measurement error calculated based on Eq. 14 is about 59 μm. The predicted error curve after truing with the compensation of measurement error of the truing wheel is shown as the red curve in Fig. 12c; it has been compensated in the next truing cycle.

The actual residual error curve after the third truing cycle is shown as the black curve in Fig. 12c. The profile error had been improved dramatically after two compensation truing cycles. The shape of this error curve is similar with the prediction model of tool setting error of y axis. The tool setting error of y axis was solved, which is about 263 μm, by fitting the error curve based on Eq. 9. The predicted error curve after truing with the compensation of this error is shown as the red

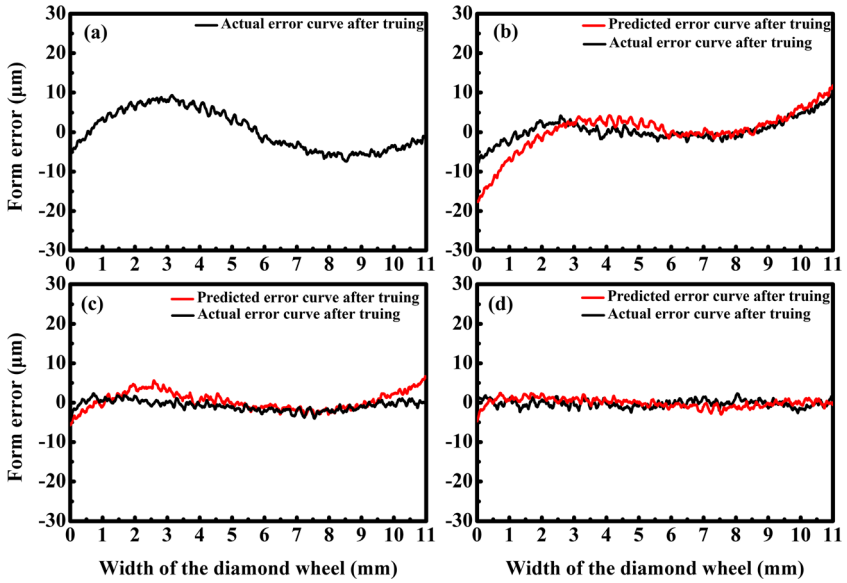

Fig. 12 Wheel profile error curves at the different stages of error compensation truing experiment **a** after the first truing cycle, **b** after the second truing cycle, **c** after the third truing cycle, and **d** after the fourth truing cycle

curve in Fig. 12d. The error was compensated in the next truing process.

At last, profile error (in PV) of diamond grinding wheel after compensation truing processes was reduced to 5 μm from 19 μm of the first truing cycle, which is shown as the black curve in Fig. 12d, and the error is well-distributed.

4.3 Surface morphology of the diamond grinding wheel

The surface morphologies of the diamond grinding wheel received from manufacture are indicated in Fig. 13. As shown in Fig. 13a, there were almost no abrasive grains protruding on the surface of the diamond grinding wheel before truing. As shown in Fig. 13b, a number of diamond grains are obviously protruding from resinoid bond after truing. The diamond grains are also well distributed on the wheel surface. The comparison of wheel surface morphologies indicated that good dressing results could also be obtained by the truing method proposed in this paper.

4.4 Form error of ground aspheric surface

The fused silica workpiece with an ellipsoidal surface after precision grinding is shown in Fig. 14a. The surface of the fused silica before the precision grinding experiments was an ellipsoidal surface generated by coarse grinding process. Form error (in PV) of the fused silica section along the width direction of the fused silica workpiece before precision grinding was 15 μm, which is shown as the black curve in Fig. 14b. After precision grinding with the grinding wheel trued by the precision helical interpolation truing method

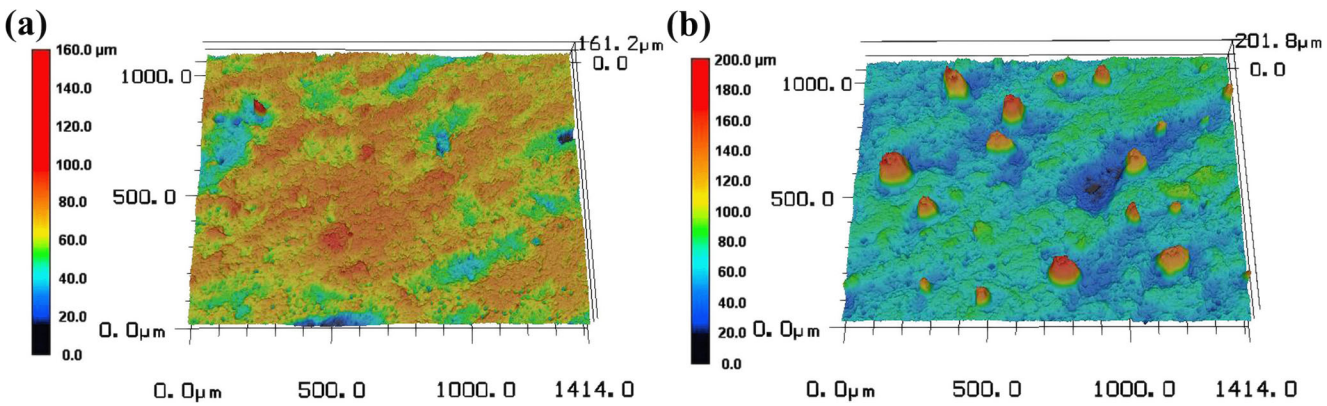

Fig. 13 Surface morphologies of the diamond grinding wheel **a** before truing and **b** after truing

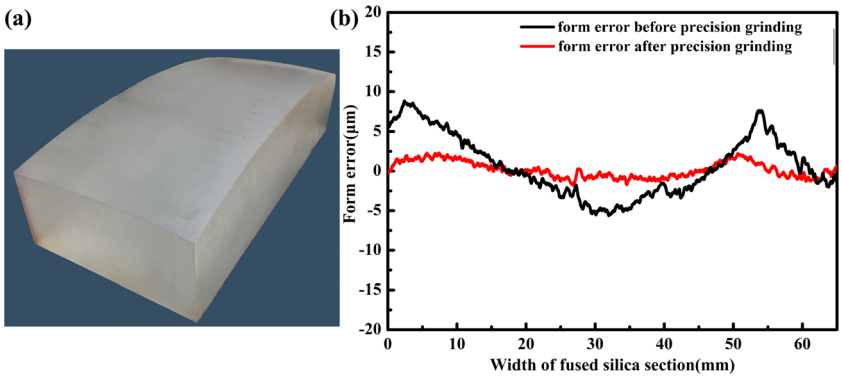

Fig. 14 **a** Fused silica workpiece with ellipsoidal surface after grinding. **b** Form error of fused silica section before and after precision grinding

and error compensation truing cycles, form error (in PV) of the fused silica section in the same direction was reduced 70% to 4.5 μm. Therefore, the form accuracy was improved dramatically by precision grinding with a well-trued grinding wheel.

5 Conclusion

To improve the precision and efficiency of free form surface generation of optical elements, the profile of arc-shaped diamond grinding wheel was proposed to be processed precisely and efficiently by the helical interpolation precision truing method in this paper. The following conclusions can by drawn.

(1) In the process of helical interpolation truing, there are many error sources that lead to profile error of grinding wheel, in which tool setting errors of z axis and y axis and measurement error of the truing wheel radius have great influence on the truing accuracy.
(2) Mathematical prediction models of these three errors are established to reveal their effects on the profile error of grinding wheel after truing. The predicted value and variation trend of truing error, which was corrected by considering the wear of truer, coincide well with the experiment results.
(3) Based on the profile error prediction models, an error compensation truing process is proposed to obtain a high truing accuracy. The profile error (PV) of wheel arc profile after truing with error compensation can be reduced to 5 μm, and it is well distributed.
(4) After aspheric grinding by the well-trued diamond grinding wheel, PV form error of the fused silica section is reduced from 15 to 4.5 μm. The form accuracy of aspheric surface increased 70% by precision truing of diamond grinding wheel.

Funding information This work was supported by National Key R&D Program of China (Grant No. 2017YFB1301903), National Natural Science Foundation of China (No. 51875321) Shandong Province Natural Science Foundation (Grant No. ZR2018MEE019), Key Laboratory of Optical System Advanced Manufacturing Technology (Grant No. Y6SY1FJ160).

References

1. Chen FJ, Yin SH, Huang H, Ohmori H, Wang Y, Fan YF, Zhu YJ (2010) Profile error compensation in ultra-precision grinding of aspheric surfaces with on-machine measurement. Int J Mach Tool Manu 50(5):480–486
2. Brinksmeier E, Mutlugünes Y, Klocke F, Aurich JC, Shore P, Ohmori H (2010) Ultra-precision grinding. CIRP Ann-Manuf Techn 59(2):652–671
3. Jiang C, Guo Y, Li H (2013) Parallel grinding error for a noncoaxial nonaxisymmetric aspheric lens using a fixture with adjustable gradient. Int J Adv Manuf Technol 66(1–4):537–545
4. Li C, Zhang F, Ma Z, Ding Y (2017) Modeling and experiment of surface error for large-aperture aspheric SiC mirror based on residual height and wheel wear. Int J Adv Manuf Technol 91(1–4):13–24
5. Kuriyagawa T, Zahmaty MSS, Syoji K (1996) A new grinding method for aspheric ceramic mirrors. J Mater Process Technol 62(4):387–392
6. Saeki M, Kuriyagawa T, Lee JS (2001) Machining of aspherical Opto-device utilizing parallel grinding method. Aspe Annual Meeting
7. Chen F, Yin S, Ohmori H, Yu J (2013) Form error compensation in single-point inclined axis nanogrinding for small aspheric insert. Int J Adv Manuf Technol 65(1–4):433–441
8. Lin XH, Wang ZZ, Guo YB, Peng YF, Hu CL (2014) Research on the error analysis and compensation for the precision grinding of large aspheric mirror surface. Int J Adv Manuf Technol 71(1–4): 233–239
9. Liu L, Zhang F (2017) Prediction model of form error influenced by grinding wheel wear in grinding process of large-scale aspheric surface with SiC ceramics. Int J Adv Manuf Technol 88(1–4): 899–906
10. Huang H, Chen WK, Kuriyagawa T (2007) Profile error compensation approaches for parallel nanogrinding of aspherical mould inserts. Int J Mach Tool Manu 47(15):2237–2245

11. Chen B, Guo B, Zhao Q (2015) An investigation into parallel and cross grinding of aspheric surface on monocrystal silicon. Int J Adv Manuf Technol 80(5–8):737–746
12. Peng Y, Dai Y, Song C, Chen S (2016) Error analysis and compensation of line contact spherical grinding with cup-shaped wheel. Int J Adv Manuf Technol 83(1–4):293–299
13. Lin X, Guo Y, Wang Z (2013) Precision model and analysis of large axisymmetric aspheric grinding. Chin J Mech Eng 49(17):65–72
14. Guo Y (2003) Study on truing and dressing Technology for arc-Diamond Wheel. Manufacturing Technology & Machine Tool
15. Xie J (2008) Experiment on CNC arc truing of diamond grinding wheel by mutual wear. Chin J Mech Eng 44(2):102–107
16. Chen B, Guo B, Zhao Q, Wang J, Chen GE (2016) On-machine precision form truing of arc-shaped diamond wheels. J Mater Process Technol 223:65–74